Human Stromal Antigen 1 (STAG1) Cohesin Subunit SA-1

A Target Enabling Package (TEP)

Gene ID / UniProt ID / EC	10274 / Q8WVM7
Target Nominator	Mark Petronczki (Boerhinger-Ingelheim)
SGC Authors	Joseph Newman, Vittorio Katis, Opher Gileadi
Collaborating Authors	Mark Petronczki[1]
Target PI	Opher Gileadi (SGC Oxford)
Therapeutic Area(s)	Cancer
Disease Relevance	STAG1 is essential for survival of cancer cells lacking the paralogue gene STAG2
Date Approved by TEP Evaluation Group	June 10 2019
Document version	Version 1
Document version date	October 2020
Citation	10.5281/zenodo.3245308
Affiliations	1. Boehringer-Ingelheim.

USEFUL LINKS

(Please note that the inclusion of links to external sites should not be taken as an endorsement of that site by the SGC in any way)

SUMMARY OF PROJECT

Loss of function mutations in the cohesin subunit gene STAG2 are common in a variety of cancers (1). These cells become dependent on the paralogous cohesin subunit STAG1 (2-4). Mutants of STAG1 that disrupt the binding to the cohesin subunit RAD21 cannot complement the loss of STAG2. This TEP examines the druggability of STAG1 as a synthetic lethal strategy to treat *stag2* - cancers. The TEP includes crystal structures of two domains of STAG1, alone and in complex with Rad21-rderived peptides. We performed screens of a fragment library and identified small molecules bound to pockets in the two domains of STAG1. We also developed assays for binding of RAD21 peptides to STAG1, which can be used to screen for molecules that disrupt binding.

SCIENTIFIC BACKGROUND

Cohesins are ring-shaped multiprotein complexes that encircle chromosomes from G1 to late anaphase, holding together sister chromatids and ensuring proper chromosomal segregation during mitosis (1,5,6). The human mitotic cohesins are composed of a core including SMC1A, SMC3, RAD21 and either of STAG1 or STAG2 proteins. STAG1 and STAG2 are mutually exclusive and bind the complex through multiple interactions with RAD21. The X-linked STAG2 gene is mutated in a significant fraction of cancers, including more than 20% of bladder cancers, Ewing sarcoma, GBM and many other cancer types (reviewed in (1)). The mutations mostly lead to loss of the protein; additional cancer cells were found to be deficient in STAG2 expression through epigenetic mechanisms. While this common loss of function may indicate a tumour-suppressor role for STAG2, the underlying mechanism has not been identified.

STAG1 and STAG2 have been assigned some non-overlapping roles in centromeres and telomeres (7); however, the survival of cancer cells lacking STAG2 indicates that there is sufficient functional overlap to allow cell proliferation. This raises the possibility that the loss of STAG2 may create a synthetic lethality, whereby the *stag2*$^{-}$ cells become critically dependent on STAG1 for proliferation and viability. Indeed, this has been demonstrated in a number of publications (2-4), where STAG2-deficient cells lose viability when STAG1 is knocked down, while cell lines expressing STAG2 are not affected.

RESULTS – THE TEP

Proteins

Initial attempts to crystallise STAG1 using the full-length protein or construct boundaries identified from the structure of STAG2 (8) failed to produce crystals, either alone or in complex with RAD21. We therefore decided to concentrate our efforts on constructs containing regions demonstrated to be important for the RAD21 interaction in the STAG2 RAD21 complex structure. For crystallisation and assay purposes, we have cloned and expressed separately two segments of STAG1 protein, which we refer to as “Site I” (residues T86-V420) and “Site IV” (residues S459-D915) These proteins were expressed, purified and crystallised separately.

Structures

Crystal structures of STAG2 in complex with a Rad21 peptide have been previously published (PDB: 4PK7, 4PJU, 4PJW) (8). We have crystallised separately two segments of STAG1, and N-terminal region (“Site I”) and a central section (“Site IV”). The relationship of the STAG1 and STAG2 structures is shown in **Fig 1**. The site of a mutation in site IV that abolishes RAD21 binding (D797K in STAG1) is marked in green in panel B.

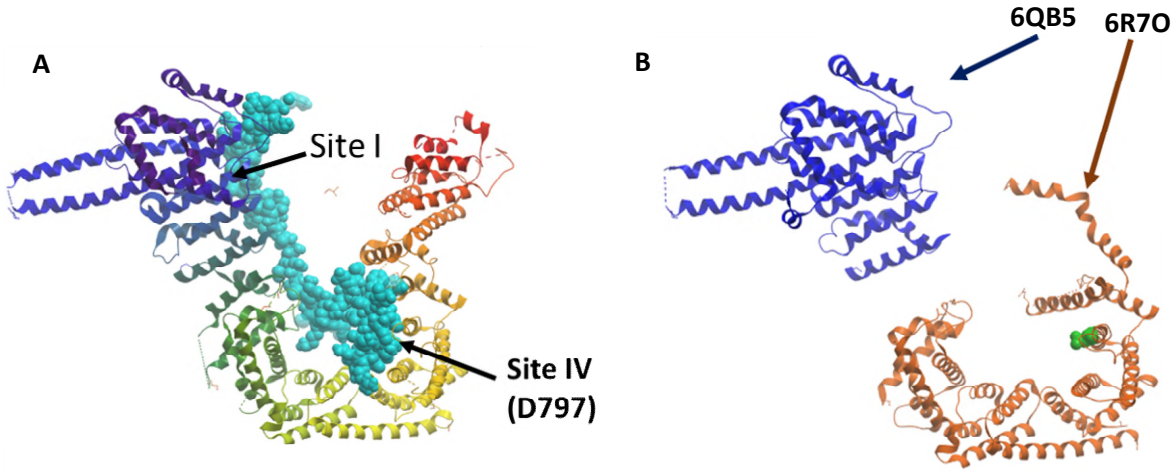

Fig. 1 (**A**) STAG2 with Rad21 (cyan) (**B**) STAG1 structures 6QB5, 6R7O

Fragment screens

Crystals of site I and site IV were soaked individually with compounds from the XChem fragment library. X-ray data was collected, and bound compounds were identified. The binding sites in both protein segments are shown in **fig. 2 and 3**; Rad21 peptides are overlaid for orientation.

Fragments bound to Site I at 4 regions, none near the peptide binding site (**fig.2**).

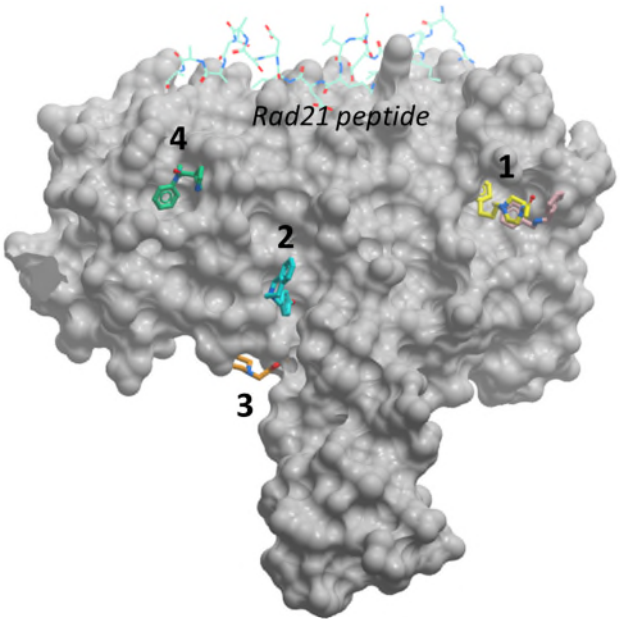

Fig. 2: Site I fragments and peptide binding

Fragments bound to site IV in two clusters, which are closer to the peptide-binding site (**fig. 3**).

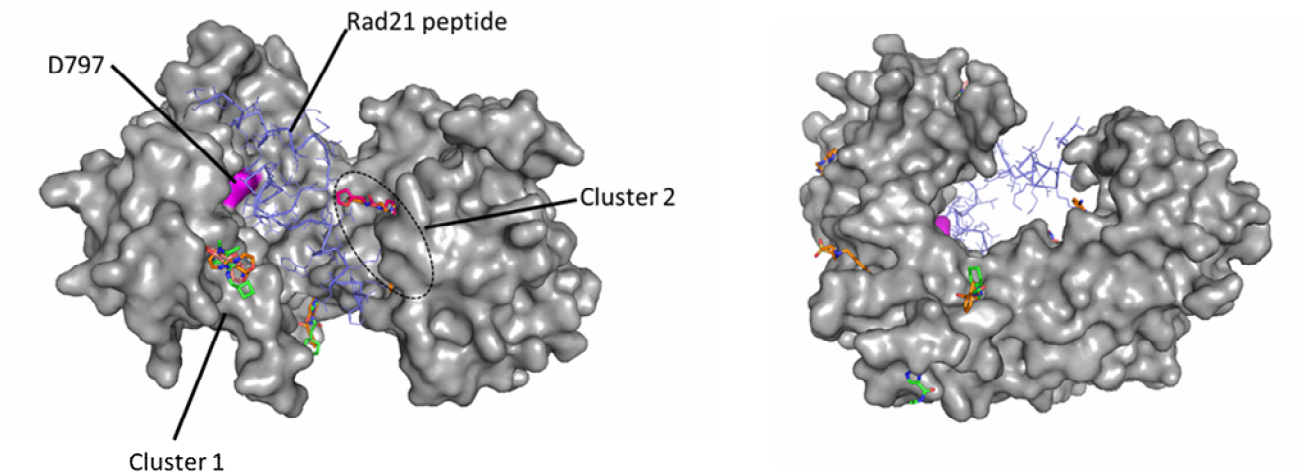

Fig. 3: Site IV fragments and peptide binding. (A) Front view (B) Bottom view

Assays

Binding of STAG1 to Rad21 peptides can be assayed using ALPHAscreen technology.

The two binding partners are STAG1 protein (Site IV, construct STAG1A-c041) with a His6 tag, and a synthetic biotinylated peptide from RAD21: Biotin-PTKKLMMWKETGGVEKLFSLPAQPLWNNRLLKLFTRCLTPL (residues 356-396). As negative controls, D797A and D797K mutants of STAG1 bind the RAD21 peptide very weakly.

Fig. 4 is a titration curve of binding at different Rad21 concentrations.

This assay can be used to measure the ability of compounds to interfere with STAG1-Rad21 binding.

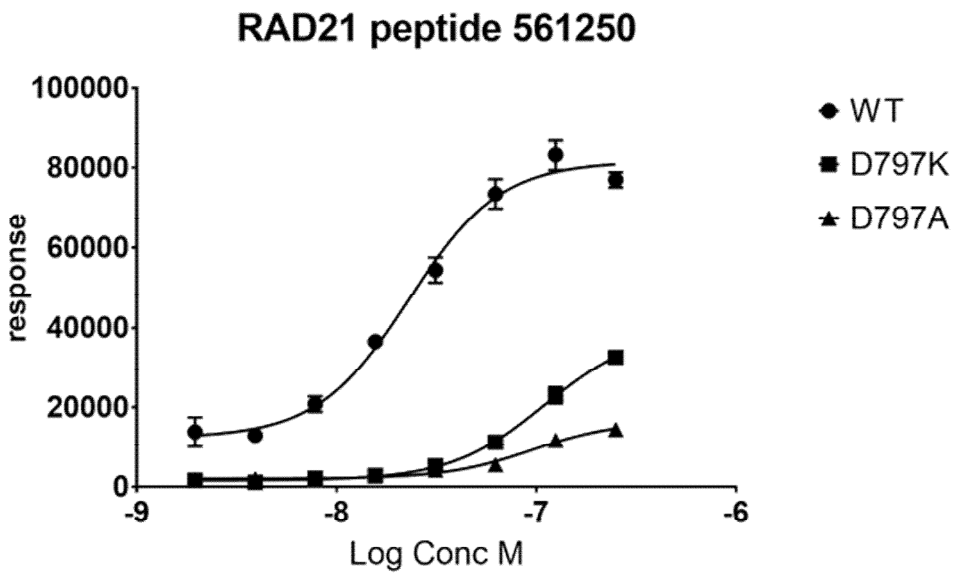

Fig. 4: ALPHAscreen assay of STAG1 (Site IV)-Rad21 binding.

Chemical Matter

PDBID	Ligand	Binding Location	Binding Pocket	Resolution (Å)
5QSY	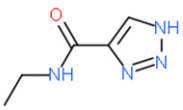 F9000425	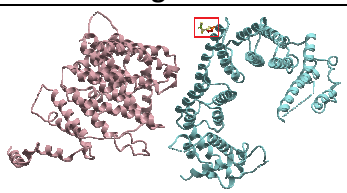 Site IV	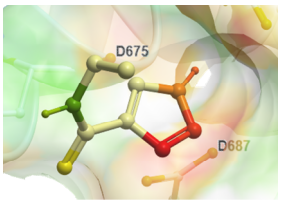	2.40
5QSZ	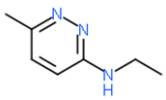 F9000428	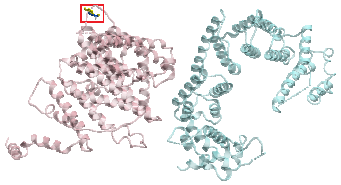 Site IV	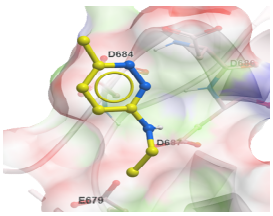	3.08
5QSM	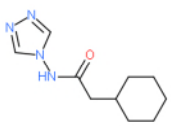 FM001876	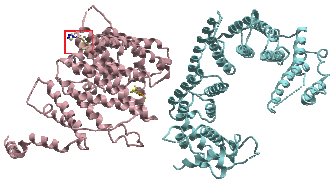 Site IV	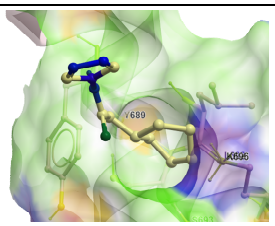	2.74
5QSN	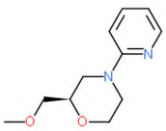 F9000495	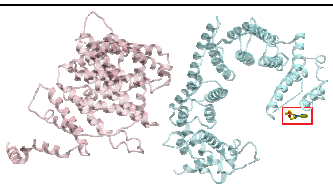 Site IV	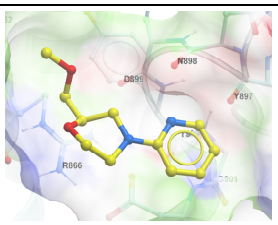	2.66

5QSO	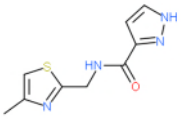 F9000338	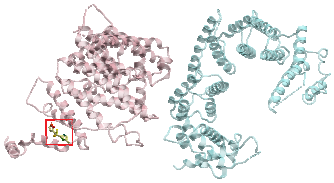 Site IV	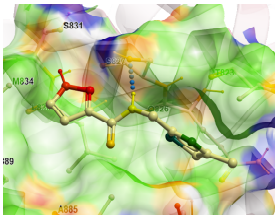	2.70
5QSP	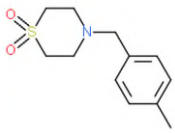 PK012938	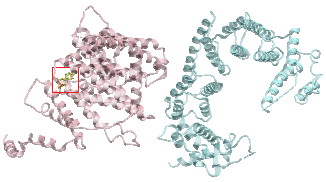 Site IV	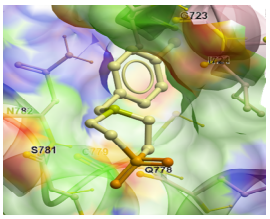	2.89
5QSQ	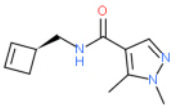 F9000948	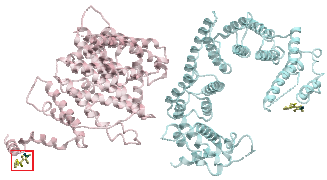 Site IV (Location 1)	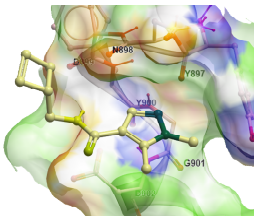 Pocket 1	2.48
		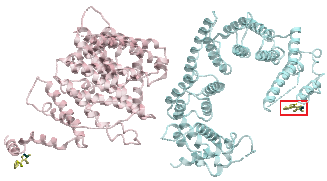 Site IV (Location 2)	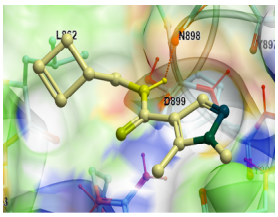 Pocket 2	
5QSR	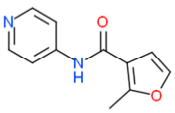 XS179878	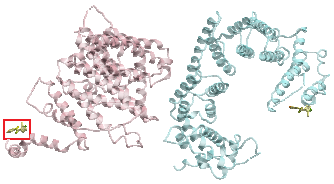 Site IV (Location 1)	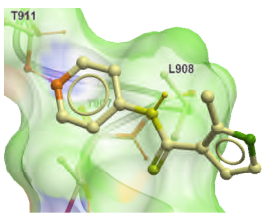 Pocket 1	3.28
		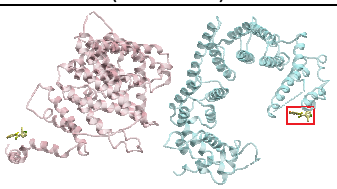 Site IV (Location 2)	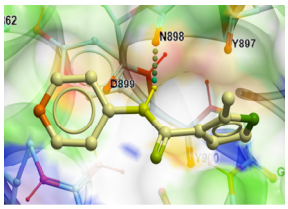 Pocket 2	
5QSS	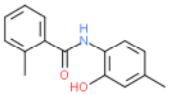 FM002161	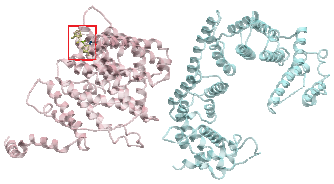 Site IV	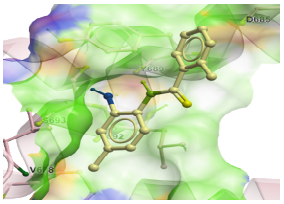	3.08

5QST	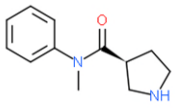 F9000447	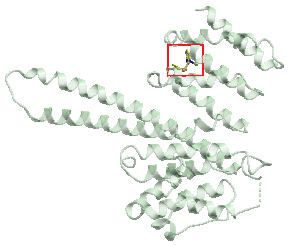 Site I	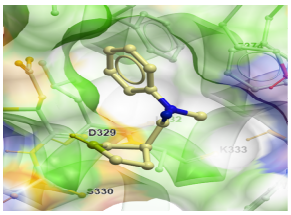	2.58
5QSU	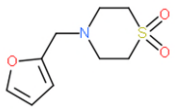 F9000364	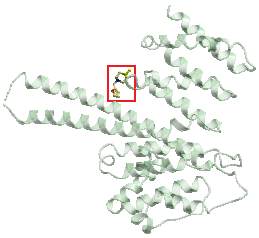 Site I	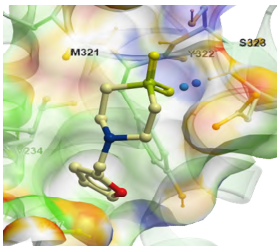	2.48
5QSV	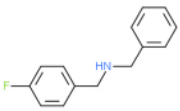 F9000377	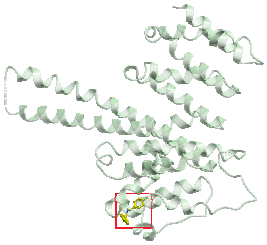 Site I	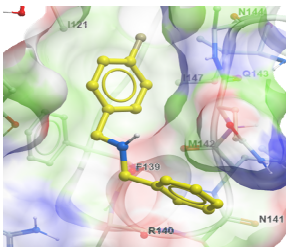	3.28
5QSW	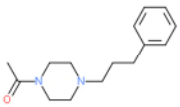 F9000400	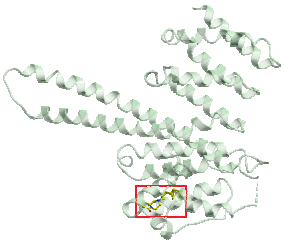 Site I	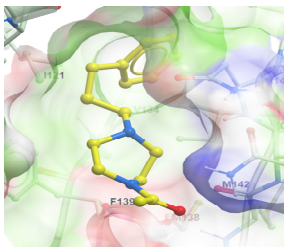	3.03
5QSX	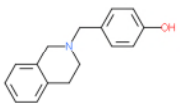 F9000348	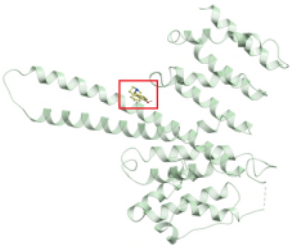 Site I	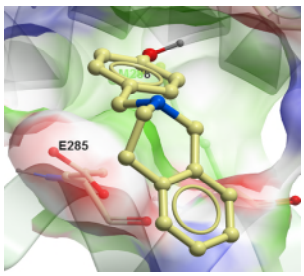	2.34

Table 1: Structures and binding sites of fragment hits

IMPORTANT: Please note that the existence of small molecules within this TEP indicates only that chemical matter might bind to the protein in potentially functionally relevant locations. The small molecule ligands are intended to be used as the basis for future chemistry optimisation to increase potency and selectivity and yield a chemical probe or lead series. As such, the molecules within this TEP should not be used as tools for functional studies of the protein, unless otherwise stated, as they are not sufficiently potent or well-characterised to be used in cellular studies.

Antibodies

Commercially available polyclonal antibody GTX129912 (GeneTex) has been validated in K/O cells for western blot and IP.

CONCLUSION

The aim of this project has been to test for the possibility of pharmacologically eliminating the STAG1-Rad21 interaction or of STAG1 protein itself. The therapeutic utility would be to utilise the vulnerability of cancers lacking functional STAG2 expression.

We have identified binding pockets in two regions of STAG1 and initial chemical matter. Some of these fragment hits may be developed into high-affinity ligands that could either interfere with Rad21 binding, or can be used as part of PROTAC molecules (9)

FUNDING INFORMATION

The work performed at the SGC has been funded by a grant from Wellcome [106169/ZZ14/Z].

ADDITIONAL INFORMATION

Structure Files

PDBID	Description	Resolution (Å)
6QB5	Crystal structure of the N-terminal region of human cohesin subunit STAG1 (Site I, aa 86 – 420)	2.02
6R7O	Crystal structure of the central region of human cohesin subunit STAG1 (Site IV, aa 459 – 915)	2.31
6RRC	Crystal structure of the N-terminal region of human cohesin subunit STAG1 in complex with RAD21 peptide (Site I, aa 86 – 420).	2.37
6RRK	Crystal structure of the central region of human cohesin subunit STAG1 in complex with RAD21 peptide (Site IV, aa 459 – 915).	3.17

Materials and Methods

Protein Expression and Purification

N-terminal region (Site 1, PDB: 6QB5 and 6RRC)
SGC Construct ID: STAG1A-c087
Protein Region: T86-V420
Vector: pNIC-ZB
Tag: N-terminal 6HIS and ZB tags followed by a TEV protease cleavage site
Host: BL21(DE3)-R3-pRARE2

Sequence (with tag(s)):
MHHHHHHSSGVDNKFNKERRRARREIRHLPNLNREQRRAFIRSLRDDPSQSANLLAEAKKLNDAQPKGTENLYFQSMGG
TLFEVVKLGKSAMQSVVDDWIESYKQDRDIALLDLINFFIQCSGCRGTVRIEMFRNMQNAEIIRKMTEEFDEDSGDYPLTM
PGPQWKKFRSNFCEFIGVLIRQCQYSIIYDEYMMDTVISLLTGLSDSQVRAFRHTSTLAAMKLMTALVNVALNLSIHQDNT
QRQYEAERNKMIGKRANERLELLLLQKRKELQENQDEIENMMNSIFKGIFVHRYRDAIAEIRAICIEEIGVVWMKMYSDAFLN
DSYLKYVGWTLHDRQGEVRLKCLKALQSLYTNRELFPKLELFTNRFKDRIVSMTLDKEYDVAVEAIRLVTLILHGSEEALSNE
DCENVYHLV

Sequence after tag cleavage:
SMGGTLFEVVKLGKSAMQSVVDDWIESYKQDRDIALLDLINFFIQCSGCRGTVRIEMFRNMQNAEIIRKMTEEFDEDSGD
YPLTMPGPQWKKFRSNFCEFIGVLIRQCQYSIIYDEYMMDTVISLLTGLSDSQVRAFRHTSTLAAMKLMTALVNVALNLSI
HQDNTQRQYEAERNKMIGKRANERLELLLLQKRKELQENQDEIENMMNSIFKGIFVHRYRDAIAEIRAICIEEIGVVWMKMY
SDAFLNDSYLKYVGWTLHDRQGEVRLKCLKALQSLYTNRELFPKLELFTNRFKDRIVSMTLDKEYDVAVEAIRLVTLILHGSE
EALSNEDCENVYHLV

DNA Sequence:
ATGCACCATCATCATCATCATTCTTCTGGTGTGGATAACAAGTTCAACAAGGAGCGTCGAAGAGCTCGCCGTGAAATT
CGCCATCTGCCGAACCTGAACCGCGAACAGCGTCGCGCATTTATTCGCAGCCTGCGCGATGATCCGAGCCAGAGCGC
GAACCTGCTGGCGGAAGCGAAGAAGCTGAACGATGCGCAGCCGAAGGGTACCGAGAACCTGTACTTCCAATCCATG
GGTGGTACATTATTTGAGGTGGTGAAACTGGGGAAAAGTGCAATGCAGTCCGTGGTGGATGACTGGATTGAATCAT
ATAAACAAGACAGGGACATCGCACTTCTGGATTTAATCAACTTTTTTATCCAGTGTTCAGGATGTCGAGGTACTGTGA
GAATAGAGATGTTTCGAAATATGCAGAATGCAGAAATCATCAGAAAAATGACTGAAGAATTTGATGAGGACAGTGG
TGATTATCCTCTTACCATGCCTGGACCTCAGTGGAAAAAATTTCGTTCAAACTTTTGTGAATTTATTGGAGTCCTGATT
CGACAGTGTCAGTATAGCATAATTTATGATGAGTATATGATGGACACAGTAATCTCCCTTTTGACGGGTTTGTCAGAC
TCCCAGGTCAGAGCTTTTAGGCATACAAGTACCCTGGCTGCCATGAAGCTCATGACTGCTCTGGTGAATGTTGCCTTA
AACCTCAGTATTCATCAGGATAATACCCAGAGACAATATGAAGCCGAGAGAAATAAAATGATTGGGAAGAGAGCCA
ATGAAAGGTTGGAGTTACTACTTCAGAAACGCAAAGAGCTGCAAGAAAATCAGGATGAAATCGAAAATATGATGAA
CTCTATTTTTAAGGGTATATTTGTTCATAGATACCGTGATGCTATTGCTGAGATTAGAGCCATTTGTATTGAAGAAATT

GGAGTATGGATGAAAATGTATAGTGATGCCTTCCTAAATGACAGTTACCTAAAATATGTTGGCTGGACTCTTCATGAC
AGGCAAGGGGAAGTCAGGCTGAAGTGTTTGAAAGCTCTGCAGAGTCTATATACCAATAGAGAATTATTCCCCAAATT
GGAACTATTCACTAACCGATTCAAGGATCGCATTGTATCAATGACACTTGATAAAGAATATGATGTTGCTGTGGAAGC
TATTCGATTGGTTACTCTGATACTTCATGGAAGTGAAGAAGCTCTTTCCAATGAAGACTGTGAAAATGTTTACCACTT
GGTG

Protein Expression
Medium: Terrific Broth (TB) Merck with 4 ml of glycerol
Antibiotics: Kanamycin

From the glycerol stock, bacteria were inoculated in 15 ml of 1 x TB in a 50 ml tube with Kanamycin 0.05 mg/ml and 0.034 mg/ml of chloramphenicol and grown overnight in a shaker at 37°C, 250rpm. The following day, 4 ml of the overnight culture were inoculated in 1L of TB. The bacteria grew in an incubator at 37°C, shaking 180 rpm. Once the OD reached 2-3, IPTG (300uM) was added to the media and left overnight at 18°C, shaking 180 rpm. The cells were harvested the following day.

Protein Purification
For purification, cell pellets were thawed and resuspended in buffer A (50 mM HEPES pH 7.5, 500 mM NaCl, 5% glycerol, 10 mM imidazole, 0.5 mM Tris (2-carboxyethyl) phosphine (TCEP)), with the addition of 1x protease inhibitor set VII (Merck, Darmstadt, Germany). Cells were lysed by sonication and cell debris pelleted by centrifugation. Lysates were loaded on to a Ni-sepharose IMAC gravity flow column (GE healthcare), washed with 2 column volumes of wash buffer (buffer A supplemented with 45 mM imidazole), and eluted with 300 mM imidazole in buffer A. The IMAC elution fraction was immediately applied to a 5ml HiTrap SP Sepharose Fast Flow column (GE healthcare), washed with 2 column volumes of elution buffer and eluted with 3 column volumes of 50 mM Hepes pH 7.5, 1 M NaCl, 5 % Glycerol. The purification tag was cleaved with the addition of 1:20 mass ratio of His-tagged TEV protease during overnight dialysis into buffer A. TEV was removed by IMAC column rebinding and final protein purification was performed by size exclusion chromatography using a HiLoad 16/60 Superdex s200 column in buffer A. Protein concentrations were determined by measurement at 280nm (Nanodrop) using the calculated molecular mass and extinction coefficients. Protein masses were checked by LC/ESI-TOF mass spectrometry (Predicted: 39581.2; observed: 39582.3).

Central region (Site IV, PDB:6R7O and 6RRK)
SGC Construct ID: STAG1A-c041
Protein Region: S459-D915
Vector: pNIC28-Bsa4
Tag: N-terminal 6HIS followed by a TEV protease cleavage site
Host: BL21(DE3)-R3-pRARE2

Sequence (with tag(s)):
MHHHHHHSSGVDLGTENLYFQSMSPNGNLIRMLVLFFLESELHEHAAYLVDSLWESSQELLKDWECMTELLLEEPVQGE
EAMSDRQESALIELMVCTIRQAAEAHPPVGRGTGKRVLTAKERKTQIDDRNKLTEHFIITLPMLLSKYSADAEKVANLLQIP
QYFDLEIYSTGRMEKHLDALLKQIKFVVEKHVESDVLEACSKTYSILCSEEYTIQNRVDIARSQLIDEFVDRFNHSVEDLLQEG
EEADDDDIYNVLSTLKRLTSFHNAHDLTKWDLFGNCYRLLKTGIEHGAMPEQIVVQALQCSHYSILWQLVKITDGSPSKED
LLVLRKTVKSFLAVCQQCLSNVNTPVKEQAFMLLCDLLMIFSHQLMTGGREGLQPLVFNPDTGLQSELLSFVMDHVFIDQ
DEENQSMEGDEEDEANKIEALHKRRNLLAAFSKLIIYDIVDMHAAADIFKHYMKYYNDYGDIIKETLSKTRQID

Sequence after tag cleavage:
SMSPNGNLIRMLVLFFLESELHEHAAYLVDSLWESSQELLKDWECMTELLLEEPVQGEEAMSDRQESALIELMVCTIRQAA
EAHPPVGRGTGKRVLTAKERKTQIDDRNKLTEHFIITLPMLLSKYSADAEKVANLLQIPQYFDLEIYSTGRMEKHLDALLKQI
KFVVEKHVESDVLEACSKTYSILCSEEYTIQNRVDIARSQLIDEFVDRFNHSVEDLLQEGEEADDDDIYNVLSTLKRLTSFHNA
HDLTKWDLFGNCYRLLKTGIEHGAMPEQIVVQALQCSHYSILWQLVKITDGSPSKEDLLVLRKTVKSFLAVCQQCLSNVNT

PVKEQAFMLLCDLLMIFSHQLMTGGREGLQPLVFNPDTGLQSELLSFVMDHVFIDQDEENQSMEGDEEDEANKIEALHK
RRNLLAAFSKLIIYDIVDMHAAADIFKHYMKYYNDYGDIIKETLSKTRQID

DNA Sequence:
CATATGCACCATCATCATCATCATTCTTCTGGTGTAGATCTGGGTACCGAGAACCTGTACTTCCAATCCATGAGCCCGA
ATGGAAACCTCATTAGGATGCTGGTTCTTTTCTTTCTTGAAAGTGAGTTACATGAACATGCAGCCTACTTGGTGGACA
GTTTATGGGAGAGCTCTCAAGAACTGTTGAAAGACTGGGAATGTATGACAGAGTTGCTATTAGAAGAACCTGTTCAA
GGAGAGGAAGCAATGTCTGATCGTCAAGAGAGTGCTCTTATAGAGCTAATGGTTTGTACAATTCGTCAAGCTGCTGA
GGCACATCCTCCAGTGGGAAGGGGTACCGGCAAGAGAGTGCTAACTGCCAAAGAAAGGAAAACTCAAATTGATGAT
AGAAACAAATTGACTGAACATTTTATTATTACACTTCCTATGTTACTGTCAAAGTATTCTGCAGATGCAGAGAAGGTA
GCAAACTTGCTACAAATCCCACAGTATTTTGATTTAGAAATCTACAGCACAGGTAGAATGGAAAAGCATCTGGATGCT
TTATTAAAACAGATTAAGTTTGTTGTGGAGAAACACGTAGAATCAGATGTTCTAGAAGCCTGCAGTAAAACCTATAGT
ATCTTATGCAGTGAAGAATATACCATCCAGAACAGAGTTGACATAGCTCGAAGCCAGCTGATTGATGAGTTTGTAGA
TCGATTCAATCATTCTGTGGAAGACCTATTGCAAGAGGGAGAAGAAGCTGATGATGATGACATTTACAATGTTCTTTC
TACATTAAAGCGGTTAACTTCTTTTCACAATGCACATGATCTCACAAAATGGGATCTCTTTGGTAATTGCTACAGATTA
TTGAAGACTGGAATTGAACATGGAGCCATGCCAGAACAGATAGTCGTGCAAGCACTGCAGTGTTCCCATTATTCGAT
TCTTTGGCAGTTGGTGAAAATTACTGATGGCTCTCCTTCCAAAGAGGATTTGTTGGTATTGAGGAAAACGGTGAAATC
CTTTTTGGCTGTTTGCCAGCAGTGCCTGTCTAATGTTAATACTCCAGTGAAAGAACAGGCTTTCATGTTACTCTGTGAT
CTTCTGATGATTTTCAGCCACCAATTAATGACAGGTGGCAGAGAGGGCCTTCAGCCTTTGGTGTTCAATCCAGATACT
GGACTCCAATCTGAACTCCTCAGTTTTGTGATGGATCACGTTTTTATTGACCAAGACGAGGAGAACCAGAGCATGGA
GGGTGATGAAGAAGATGAAGCTAATAAAATTGAGGCCTTACATAAAAGAAGGAATCTACTTGCTGCTTTCAGCAAAC
TTATCATTTATGACATTGTTGACATGCATGCAGCTGCAGACATCTTCAAACACTACATGAAGTATTACAATGACTATGG
TGATATTATTAAGGAAACACTGAGTAAAACCAGGCAGATTGATAAAATTCAGTGTGCCAAGACTCTCATTCTCAGTTT
GCAACAGTTATTTAATGAACTTGTTCAAGAGCAAGGTTGACAGTAAAGGTGGATACGGATCCGAA

Protein Expression
Medium: Terrific Broth (TB) Merck with 4 ml of glycerol
Antibiotics: Kanamycin

From the glycerol stock, bacteria were inoculated in 15 ml of 1 x TB in a 50 ml tube with Kanamycin 0.05 mg/ml and 0.034 mg/ml of chloramphenicol and grown overnight in a shaker at 37°C, 250rpm. The following day, 4 ml of the overnight culture were inoculated in 1L of TB. The bacteria grew in an incubator at 37°C, shaking 180 rpm. Once the OD reached 2-3, IPTG (300uM) was added to the media and left overnight at 18°C, shaking 180 rpm. The pellet was harvested the following day.

Protein Purification
For purification, cell pellets were thawed and resuspended in buffer A (50 mM HEPES pH 7.5, 500 mM NaCl, 5% glycerol, 10 mM imidazole, 0.5 mM Tris (2-carboxyethyl) phosphine (TCEP)), with the addition of 1x protease inhibitor set VII (Merck, Darmstadt, Germany). Cells were lysed by sonication and cell debris pelleted by centrifugation. Lysates were loaded on to a Ni-sepharose IMAC gravity flow column (GE healthcare), washed with 2 column volumes of wash buffer (buffer A supplemented with 45 mM imidazole) and eluted with 300 mM imidazole in buffer A. The purification tag was cleaved with the addition of 1:20 mass ratio of His-tagged TEV protease during overnight dialysis into buffer A. TEV was removed by IMAC column rebinding and final protein purification was performed by size exclusion chromatography using a HiLoad 16/60 Superdex s200 column in buffer A. Protein concentrations were determined by measurement at 280nm (Nanodrop) using the calculated molecular mass and extinction coefficients. Protein masses were checked by LC/ESI-TOF mass spectrometry (Predicted: 52692.1; observed: 52693.8).

Structure Determination

6QB5: Crystal structure of the N-terminal region of human cohesin subunit STAG1 (Site I, aa 86 – 420)

Crystallization: For crystallisation the protein was concentrated to 15 mg/ml and crystallised by sitting drop vapor diffusion. Crystals grew in conditions containing 0.1 M Na/K phosphate pH 6.0, 0.2 M NaCl, 34% PEG200. Initial crystals were substantially improved by seeding using a 1000-fold dilution of seed stock. Crystals were loop mounted and cryo-cooled by plunging directly into liquid nitrogen.

Data Collection: Data were collected to 2.0 Å resolution at Diamond light source beamline I04-1 and processed using DIALS.

Data Processing: Structures were solved by molecular replacement using the programme PHASER and the structure of the STAG2 SCC1 complex (4PK7) as a search model. The structure was refined using PHENIX REFINE to a final Rfactor = 21.8%, Rfree = 24.5%.

6R7O: Crystal structure of the central region of human cohesin subunit STAG1 (Site IV, aa 459 – 915)
Crystallisation: For crystallisation the protein was concentrated to 5 mg/ml and crystallised by sitting drop vapour diffusion from conditions containing 20 % PEG 3350, 10 % ethylene glycol, 0.2 M sodium malonate, 0.1 M Bis-Tris Propane pH 7.0. Crystals were loop mounted and cryo-cooled by plunging directly into liquid nitrogen.

Data Collection: Data were collected to 2.3 Å resolution at Diamond light source beamline I04-1 and processed using DIALS.

Data Processing: Structures were solved by Molecular replacement using the programme PHASER and the structure of the STAG2 SCC1 complex (4PK7) as a search model. The structure was refined using PHENIX REFINE to a final Rfactor = 22.6 %, Rfree = 26.4 %

6RRC: Crystal structure of the N-terminal region of human cohesin subunit STAG1 in complex with RAD21 peptide (Site I, aa 86 – 420)
Crystallization: For crystallization, a SCC1 peptide corresponding to the sequence KRKLIVDSVKELDSKTIRAQLSDYS was mixed with the protein in a 1:1 ratio and crystallization trials were set up at 12 mg/ml. The peptide bound crystals appeared in conditions containing 2.1 M Ammonium Sulfate, 0.1 M MES pH 6.3. Crystals were transferred to a cryo solution containing well solution supplemented with 25 % Glycerol before being loop mounted and plunged into liquid nitrogen.

Data Collection: Data were collected to 2.4 Å resolution at Diamond light source beamline I04-1, and processed using DIALS.

Data Processing: Structures were solved by Molecular replacement using the programme PHASER and the structure of the STAG2 SCC1 complex (4PK7) as a search model. The structure was refined using PHENIX REFINE to a final Rfactor = 21.4%, Rfree = 24%

6RRK: Crystal structure of the central region of human cohesin subunit STAG1 in complex with RAD21 peptide (Site IV, aa 459 – 915)
Crystallisation: For crystallisation of the Site IV peptide bound crystals, a SCC1 peptide corresponding to the sequence PTKKLMMWKETGGVEKLFSLPAQPLWNNRLLKLFTRCLTP was mixed with the protein in a 1:1 ratio and crystallisation trials were set up at 8.5 mg/ml. Crystals grew from conditions containing 16 % PEG 3350, 0.2 M DL-Malic acid. Crystals were loop mounted and transferred to a cryo solution containing well solution supplemented with 20 % ethylene glycol before being loop mounted and plunged into liquid nitrogen.

Data Collection: Data were collected to 3.2 Å resolution at Diamond light source beamline I24 and processed using DIALS.

Data Processing: Structures were solved by Molecular replacement using the programme PHASER and the structure of the STAG2 SCC1 complex (4PK7) as a search model. The structure was refined using PHENIX REFINE to a final Rfactor = 21.9 %, Rfree = 27.8%

Assays

Alphascreen assay

An alphascreen binding assay was developed using streptavidin alphascreen donor beads and Ni-NTA alphascreen acceptor beads. The assay was performed in 384 well format plates with histidine tagged STAG1A-c041 and a synthetic biotinylated peptide from Rad 21: Biotin-PTKKLMMWKETGGVEKLFSLPAQPLWNNRLLKLFTRCLTPL (residues 356-396). Both protein and peptide were diluted in a buffer containing 25 mM HEPES pH 7.4, 100 mM NaCl, 0.1 % BSA, 0.01 % CHAPS. The assay format was 4µl Buffer + 4µl Protein + 4ul Peptide. Reactions were incubated for 20 minutes and 8 µl of bead mixture was added (1:600 dilution of both beads). The plate was measured after further incubation for 2 hours using a PHERAstar FSX plate reader using excitation and emission wavelengths of 680 and 570 nm.

References

1. Hill, V. K., Kim, J. S., and Waldman, T. (2016) Cohesin mutations in human cancer. *Biochim Biophys WActa* **1866**, 1-11
2. Benedetti, L., Cereda, M., Monteverde, L., Desai, N., and Ciccarelli, F. D. (2017) Synthetic lethal interaction between the tumour suppressor STAG2 and its paralog STAG1. *Oncotarget* **8**, 37619-37632
3. Mondal, G., Stevers, M., Goode, B., Ashworth, A., and Solomon, D. A. (2019) A requirement for STAG2 in replication fork progression creates a targetable synthetic lethality in cohesin-mutant cancers. *Nat Commun* **10**, 1686
4. van der Lelij, P., Lieb, S., Jude, J., Wutz, G., Santos, C. P., Falkenberg, K., Schlattl, A., Ban, J., Schwentner, R., Hoffmann, T., Kovar, H., Real, F. X., Waldman, T., Pearson, M. A., Kraut, N., Peters, J. M., Zuber, J., and Petronczki, M. (2017) Synthetic lethality between the cohesin subunits STAG1 and STAG2 in diverse cancer contexts. *Elife* **6**
5. Losada, A. (2014) Cohesin in cancer: chromosome segregation and beyond. *Nat Rev Cancer* **14**, 389-393
6. Michaelis, C., Ciosk, R., and Nasmyth, K. (1997) Cohesins: chromosomal proteins that prevent premature separation of sister chromatids. *Cell* **91**, 35-45
7. Canudas, S., and Smith, S. (2009) Differential regulation of telomere and centromere cohesion by the Scc3 homologues SA1 and SA2, respectively, in human cells. *J Cell Biol* **187**, 165-173
8. Hara, K., Zheng, G., Qu, Q., Liu, H., Ouyang, Z., Chen, Z., Tomchick, D. R., and Yu, H. (2014) Structure of cohesin subcomplex pinpoints direct shugoshin-Wapl antagonism in centromeric cohesion. *Nat Struct Mol Biol* **21**, 864-870
9. Sakamoto, K. M., Kim, K. B., Kumagai, A., Mercurio, F., Crews, C. M., and Deshaies, R. J. (2001) Protacs: chimeric molecules that target proteins to the Skp1-Cullin-F box complex for ubiquitination and degradation. *Proc Natl Acad Sci U S A* **98**, 8554-8559
10. van der Lelij, P., Newman, J. A., Lieb, S., Jude, J., Katis, V., Hoffmann, T., Hinterndorfer, M., Bader, G., Kraut, N., PEarson, M. A., Peters, J., Zuber, J., Gileadi, O., and Petronczki, M. (2020) STAG1 vulnerabilities for exploiting cohesin synthetic lethality in STAG2-deficient cancers. *Life Sci Alliance* **28,** 3(7)

We respectfully request that this document is cited using the DOI value as given above if the content is used in your work.